ISSN 2706-655X Vol.3, Issue 9: 56-65, DOI: 10.25236/IJFET.2021.030910

Loading-Unloading Mechanical Characteristics and Constitutive Model of Porous Rock

Zhe Liu[a*], Jiajing Li[b], Wei Wang[c]

School of Petroleum Engineering, Guangdong University of Petrochemical Technology, Maoming 525000, Guangdong, China
[a] liuzhe@gdupt.edu.cn, [b] lijiajing@gdupt.edu.cn, [c] 381583142@qq.com
**Corresponding author*

Abstract: *This paper studies the stress-strain relationship of rock in the process of loading and unloading. Taking sandstone as an example, conventional triaxial loading and unloading experiments are carried out. The non-linear characteristics of rock during the post-peak unloading stage are analyzed, and the damage variable of rock is defined. An elastic modulus model for describing the stress-strain relationship during post-peak unloading is presented. The relationship between the axial strain and the radial strain in the loading-unloading process is analyzed; the Poisson's ratio model in unloading process is obtained. The D-P plastic model is introduced to modify the hardening function according to the plastic hardening characteristics of sandstone; a damage model associated with equivalent plastic strain is established. The computational model is matrixed and then calculated numerically. In the process, the following conclusions are drawn: (1) The porous rock shows obvious non-linear characteristics during loading. With the increase of body stress, the elastic modulus of rock increases gradually. (2) When the axial stress is greater than the confining pressure in the process of unloading rock after peak load, Stress-strain can be described by multiplying the elastic modulus model of the pre-peak elastic stage by the continuity factor. (3) With the increase of equivalent plastic strain, Poisson's ratio increases first, then decreases, and finally tends to be stable. In the post-peak unloading process, the equivalent plastic strain does not change, while the Poisson's ratio remains unchanged. The results show that the proposed model can reflect the stress-strain law of rock during post-peak unloading.*

Keywords: *Rock Mechanics, Stress-Strain Relationship, Modulus of Elasticity*

1. Introduction

The rock mass is a geological structure composed of a structural plane and a complete rock mass, and is compatible with general media. The main difference is that it is a multi-cracked body with a specific structure cut by many structural planes. Structural surfaces, also known as discontinuous surfaces, are a general term for geological interfaces that rupture or are prone to cracking in rock mass with no or only very low tensile strength. It includes joints, faults, bedding and weak surfaces, where the joint is the most widely developed structural surface in rock mass. The presence of the joint results in a reduction in the effective bearing area of the rock mass and a reduction in mechanical properties. The deformation characteristics and mechanical properties of the intact rock mass and joint plane determine the strength and deformation failure characteristics of the whole jointed rock mass [1]. With the rapid development of human society and the continuous advancement of science and technology, the demand for resources and energy has further increased. The reduction of shallow resources has led to the further development of the exploitation of resources in various countries [2]. Deep resource development is the excavation of deep rock masses, forming a certain free space (well and diverticulum). The deep underground ore is then extracted and transported to the ground by human and mechanical means. During the deep exploitation of resources, the stresses on the free faces of the wells, diverticulum and goaf are redistributed. Stress concentration occurs, and the surrounding rock deformation is significant, directly affecting the long-term stability of the project and the safety of personnel and property. The deep engineering rock mass has high ground stress, high osmotic pressure, high temperature and strong mining disturbance, and the “three highs and one disturbance” [3] complex mechanical environment. The mechanical properties and deformation and failure characteristics of the rock mass are affected by the complex geomechanical environment. The impact is very different from the shallow rock mass. It exhibits distinct rock deformation characteristics, deformation and rheology

ISSN 2706-655X Vol.3, Issue 9: 56-65, DOI: 10.25236/IJFET.2021.030910

time dependence, and transition from brittleness to toughness. First, the rock mass exhibits different post-peak characteristics under different confining pressure conditions, and the total strain at the time of the final failure is also different [4]. The deep underground rock mass is in high stress and high confining pressure environment, and the rock is characterized by ductile failure and final plastic deformation and deformation. Secondly, a prominent feature of deep rock mass engineering is that the ground temperature is high, and the deeper the ground, the higher the ground temperature [5]. Studies have shown that when the local temperature is low, the fracture strain of the rock mass is very small, and it is difficult to produce lattice slip. The rock mass will generate structural thermal stress. As a result, the rock mass undergoes large permanent plastic deformation under pressure and the strength is reduced, which is more likely to be toughness damage. Third, due to the low engineering load, surface or shallow geological soft rock is not easy to produce obvious plastic deformation. It is not considered to be an engineering soft rock. Even some geological hard rockes have significant plastic deformation and significant rheological properties. Therefore, the concept of softening the critical depth in the depth of the underground is proposed. Finally, groundwater affects the mechanical properties and deformation and failure characteristics of rocks through physical and chemical interactions and hydraulic interactions. After the physical and chemical reactions of water and rock, the mineral composition of the rock in the water environment changes, the microstructure changes, the volume expands, and micropores and microcracks are generated. Porosity increases, microcracks expand, rock damage increases, permeability and pore pressure increase, resulting in reduced effective stress and reduced friction coefficient of rock mass joints. The ability of the rock mass to resist damage is weakened, and the macroscopic strength and stiffness of the rock mass are further reduced. In addition, the weakening of the internal structure of the deep rock mass and the weakening of the mechanical properties of the groundwater reduce the long-term strength of the rock mass. Creep deformation, creep rate and creep duration increase, which exacerbates the rheological properties of deep rock masses.

Wang R found that there are significant differences in the mechanical properties of jointed rock mass under loading and unloading conditions [6]. However, there are relatively few studies on the damage characteristics of jointed rock mass under unloading conditions, especially the influence of different unloading degree on the mechanical properties of jointed rock mass. In order to understand the unloading degree, the influence of joint inclination and confining pressure on the deformation characteristics of rock mass, repeated load tests were carried out in the laboratory. The results show that as the unloading value increases, the peak intensity decreases. When the unloading degree is low, it has little effect on the ultimate strength of the rock mass. As the unloading value increases, the decrease in the ultimate strength of the rock increases. Under the condition of low confining pressure, the characteristics of brittle stress drop are obvious. With the increase of confining pressure, the deformation of rock mass from failure to residual strength increases, and the influence of unloading degree on the mechanical properties of rock mass is gradually reduced. The combined dip and degree of unloading have a large effect on the Poisson's ratio. The Poisson's ratio of the jointed rock sample is greater than the Poisson's ratio of the intact rock sample, reaching a maximum when the joint inclination angle is 45°. The Poisson's ratio increases with the degree of unloading, and the higher the degree of unloading, the faster the rate of increase of Poisson's ratio. Confining pressure, joint inclination and unloading damage are related to the elastic modulus of jointed rock mass. As the confining pressure increases, the elastic modulus value increases but the rate of increase decreases. The degree of reduction in the modulus of elasticity increases as the degree of unloading increases. In addition, for rock samples with different inclination angles, the influence of the degree of unloading on the modulus of elasticity is different, and the rock samples with the inclination angles of 45° and 60° have the greatest influence. Under the deep and complex geological conditions of large depth, the disturbance caused by the excavation of surrounding rock structure in underground mining is caused by stress concentration and unloading [7], resulting in rock failure. Therefore, the design, construction, and maintenance of structures struts, drifts, chambers are based not only on peak strength, but also on post-peak behavior and subsequent residual rock strength. Therefore, a better understanding of the characteristics of the rock in the post-peak stage is critical for underground construction and ground support design activities. At different initial confining pressures, the argillaceous limestone samples loaded into the residual phase in a conventional triaxial compression test were continuously loaded by loading and unloading cycles [8].

Acoustic emission (AE) monitoring is used to supplement the analysis of the variation characteristics of stress and strain to study the effects of confining pressure and loading and unloading cycles on the mechanical properties of rocks in the residual phase. In addition, the yield warning information of the rock in the confining pressure stage is analyzed and calculated [9]. The results show that the axial load deformation mainly comes from the sliding between the fracture surfaces, and the

ISSN 2706-655X Vol.3, Issue 9: 56-65, DOI: 10.25236/IJFET.2021.030910

bearing capacity is not only related to the confining pressure, but also related to the unloading path; the elastic modulus of the axial elastic deformation stage is greater than the corresponding elastic modulus of the prefabrication stage, the axis The deformation has good elastoplastic deformation characteristics; the frictional sliding between elastic blocks under confining pressure provides the bearing capacity of the rock in the residual phase. According to the evolution characteristics of the AE amplitude, the precursor information of the yield plastic deformation of the rock in the rock compression confining test can be determined. Dong X used the YAG-3000 microcomputer to control the rock stiffness tester and the PCI-II acoustic emission monitoring system [10], and carried out cyclic loading tests on the dry and water-saturated diorite of Zhongguan Iron Mine, and analyzed the mechanical properties and acoustic emission characteristics. The change. The results show that the water content has a significant effect on rock strength and acoustic emission properties. The compressive strength of the water-saturated sample was 6.96% lower than that of the dried sample; the cumulative AE event of water saturation accounted for 17.94% of the dry sample throughout the process, and the total AE event of the water-saturated sample was approximately the dry sample before the peak. 4.6% [11]. In addition, the maximum LURR of the dried sample occurs before the intensity value, while the maximum LURR of the water-saturated sample occurs during the unstable extension of the fracture.

In this paper, the nonlinear characteristics of rock in the post-peak unloading stage are analyzed, and the damage variable of rock is defined. The elastic modulus model used to describe the stress-strain relationship in the post-peak unloading process is given. By analyzing the relationship between axial strain and radial strain during loading-unloading, the Poisson's ratio model during unloading is obtained. The D-P plasticity model was introduced. The hardening function was modified for the plastic hardening characteristics of sandstone, and the damage model associated with equivalent plastic strain was established. The calculation model is matrixed and then numerically calculated. In this process, the following conclusions are obtained: (1) The porous rock exhibits obvious nonlinear characteristics during the loading process. With the increase of the bulk stress, the elastic modulus of the rock increases gradually. (2) During the post-peak unloading process, when the axial stress is greater than the confining pressure, the stress-strain can be described by multiplying the elastic modulus model of the pre-peak elastic stage by the continuity factor. (3) With the increase of the equivalent plastic strain, the Poisson's ratio first increases and then decreases, and finally tends to be stable. During the post-peak unloading process, the equivalent plastic strain does not change, and the Poisson's ratio remains unchanged. The results show that the model proposed in this paper can reflect the stress-strain law of rock during the post-peak unloading process.

2. Proposed Method

2.1 Rock Mechanics Characteristics

Rock mechanics is increasingly important as a discipline of national economic development. Rock mechanics is a branch of mechanics. Rock mechanics is the discipline of understanding and controlling rocks. There are all kinds of rocks in nature, each with its mechanical properties. In terms of geology, it can be divided into three categories according to its causes: magmatic rocks, sedimentary rocks and metamorphic rocks. Rocks are natural aggregates produced by the geological interaction of one or more minerals with a certain connection. The basic composition of rock is determined by diagenetic minerals and structural planes. The rock-forming minerals of the rock are: primitive, amphibole, quartz, calcite, biotite, kaolinite, pyroxene, peridot, etc. Due to the content of diagenetic minerals, rocks of different origins are different. The relationship between mineral particles constitutes the structure of the rock. The main types of rock structure connections are crystallization and cementation. The crystal bond is a mineral particle inlaid with crystals. Bonded joints are bonded together by cement, including matrix bonding, contact bonding, and pore cementing. The strength of the rock depends mainly on the type of cement and the type of cement. The internal defects of the rock seriously affect the strength of the rock. Mainly mineral cracking, grain boundaries, lattice defects, microcracks, etc. The rock is complex and varied. Mainly have bulk density, specific gravity, porosity and so on. Heterogeneity, discontinuity and anisotropy are the basic characteristics of petrophysical properties.

(1) Rock heterogeneity

Rocks continue to evolve under the influence of geology. The material composition of the rock continues to produce weak components, and there are phenomena such as displacement, vacancies, interlayers and other substances in the rock. Make the original structure produce a discontinuous surface. The same lithologic rock in the same area has different physical and mechanical properties.

ISSN 2706-655X Vol.3, Issue 9: 56-65, DOI: 10.25236/IJFET.2021.030910

Rocks are affected by natural and human factors, and there are various macroscopic, microscopic and structurally weak surfaces in the rock. The physical properties of rocks are more uneven, and the weak surfaces of these cracks and structures greatly reduce the mechanical strength of the rock. Even rocks with small particle sizes are not uniform, and rocks with a small degree of blockiness also contain fragile crystals or particles, weaker minerals and cement. Under the action of external force, weathering or local erosion makes the rock more fragile, resulting in mineral crystallization in the rock, intergranular contact surface expansion and microcracking. The rock softening process is a process of rock heterogeneity.

(2) Rock discontinuity

During geological evolution, rocks form different types of structural surfaces, including interfaces, fractures, and fillers between various rocks. These constitute discontinuities in the physical properties of the rock and affect the continuous distribution of the rock. The rock interface and cracks are densely distributed, with long extension time and weak rock continuity. Similar discontinuous rocks have different characteristics due to the nature of the crack surface.

(3) Anisotropy of rock

Since the distribution of different kinds of components in the rock is oriented, the rock is anisotropic. The anisotropy of rock is the basic property of rock and an important characteristic of rock mass. The anisotropy of rock means that some or all of the physical and mechanical properties of the rock exhibit different phenomena in different directions. When the rock is loaded in different directions, the rock exhibits different deformation characteristics, different elastic moduli, different Poisson's ratios and different strength characteristics. The genesis of rock anisotropy and its different manifestations can be divided into primary and secondary anisotropy. In the process of diagenesis, due to the arrangement of mineral particles in different directions in rock, the difference between rock parameters and mechanical properties is called rock main anisotropy. As the stress state of the rock changes, the different stress directions of the rock stress produce different deformation characteristics in all directions. The main anisotropy of rock is mainly a description of the physical parameters of the rock and the intrinsic properties of the rock. The secondary anisotropy of rock is mainly caused by the change of rock stress and the deformation law in different directions. The anisotropy of a rock can be expressed by an anisotropic coefficient, expressed as the ratio of the weakest direction of the physical and mechanical parameters of the rock to the strongest direction of the physical and mechanical parameters. The anisotropy coefficients produced by different parameters are also different.

2.2 Factors Affecting the Mechanical Properties of Rock

(1) Influence of rock structure

Different rocks contain different components and their mechanical properties are completely different. The internal hardness of the rock is high, the content is high, and the rock strength is large; if the particle hardness is small and the content is large, the strength of the rock is smaller. Under the action of geology, there are different structural planes inside the rock, and there are cracks inside the rock, which affects the mechanical properties of the rock. As the pressure increases, the shrinkage of the rock decreases. As the pressure increases, the porosity of the rock decreases. The length of the crack is a decisive factor affecting rock shrinkage. Cracks inside the rock are important factors affecting rock anisotropy.

(2) The influence of water

When the rock encounters water, it will cause changes in various properties of the rock. Water is present in the rock, in a state where water and free water combine. The bound water in the rock is water on the surface of the rock particles. Connecting the particles within the rock to each other results in a reduction in friction between the particles within the rock, causing the water molecules to squeeze into the cracks between the rock particles. These effects expand the volume of the rock and create an expansion force that reduces the strength of the rock. The water in the rock takes away the fine particles in the pores of the rock, increasing the deformation of the rock and reducing the strength of the rock. The water in the rock has an effect on the elastic modulus and Poisson's ratio of the rock. The pore water of the rock has a great influence on the deformation characteristics of the rock.

(3) Influence of confining pressure

As the depth of the rock increases, the water absorption and porosity of the rock will decrease, the

ISSN 2706-655X Vol.3, Issue 9: 56-65, DOI: 10.25236/IJFET.2021.030910

cohesion and shear strength of the rock will increase significantly, and the internal friction angle of the rock will not change significantly. The compressive strength of the rock increases, the elastic modulus of the rock increases significantly, and the Poisson's ratio of the rock decreases. The rock is underground and the surrounding rocks put pressure on it:

$$P = \gamma H = \rho g H \tag{1}$$

Where: —— the bulk density of the overburden;

H - The depth of the rock.

As the rock confining pressure increases, the compressive strength of the rock increases, the elastic modulus of the rock does not change, and the Poisson's ratio of the rock increases. The deformation modulus of the rock increases first and then decreases. The strain before the rock breaks also increases, the plasticity of the rock increases, and the rock changes from brittle to ductile.

3. Experiments

3.1 Experimental Test Piece Production

The composition of the rock slurry is rock particles, water and cement. The rock particles from the experimental preparation of the rock slurry are derived from the borehole of the mining road in the lower mining area of the Weinan Coal Mine in the Yubei Mining Area, and then the different rock particle sizes are obtained through processing and screening. The cement is made of P.O42.5 ordinary Portland cement. The water slurry ratio of the prepared rock slurry specimen is 0.5:1, and the rock particles are divided into 2.5 mm to 5 mm, 5 mm to 10 mm, and 10 mm to 20 mm. At the time of manufacture, the drilled core is chopped and then sieved through a standard rock screen. According to the water-cement ratio, the cement slurry and the rock particles of different diameters are evenly stirred, and then poured into a standard mold for consolidation. After 1 week, the mold was removed and dried, and watering was carried out in the process. In order to process it into a standard part, it was cut and polished into a standard cylindrical test piece of φ50 mm×100 mm after 30 days.

3.2 Experimental Design

The vertical stress of the two gangs is in a process of equilibrium-redistribution-balance. The vertical stress is regarded as the axial pressure, the horizontal stress is regarded as the confining pressure, the lane gang is the one confining pressure, and the axial compression cycle the process of loading and unloading. The test instrument adopts RMT-150B, which mainly adopts the test method of increasing ($\sigma_1 - \sigma_3$) difference in stress control mode (σ_1 is axial stress, σ_3 is confining pressure), and cyclic loading and unloading axial pressure is performed by fixed confining pressure. The test was operated using manual control. The specific process of the test is as follows.

(1) The axial stress was applied at a rate of 0.1 kN/s, and the confining pressure was loaded at a rate of 0.05 MPa/s. The axial stress and the confining pressure are simultaneously performed and loaded to a hydrostatic state at a predetermined value. (2) The confining pressure is kept constant, and the axial stress is gradually applied to the stress state at a rate of 0.2 kN/s before the test piece is broken. The stress state is set to 80% of the average strength of the conventional triaxial compression test. (3) Keep the confining pressure constant and eliminate the axial stress at a speed of 0.2 kN/s. When the shaft pressure is unloaded to the set value, the next stage load is immediately set to the same rate. Observe the strain rate of the test curve and end the load when the strain rate is significantly accelerated. Start setting the next level of load until the test piece is disconnected. According to the upper limit load, the setting of the next stage load is increased by 10%.

4. Discussion

4.1 Process Analysis

(1) Rockman207 rock triaxial test machine was selected as the experimental equipment and rock sample preparation test machine. The computer can precisely control the entire test process through deformation control and load control. As a result, the Rockman 207, which is highly calibrated,

ISSN 2706-655X Vol.3, Issue 9: 56-65, DOI: 10.25236/IJFET.2021.030910

performs all aspects of rock mechanical testing and provides highly reliable test data. The maximum axial force output is 2000kN and the maximum confining pressure is 70MPa. The device uses an ultra-small displacement sensor manufactured by MicroInc., USA to measure axial deformation. The measuring range of the sensor is 0mm to 2mm with an accuracy of 0.05%. The hard rock samples required for the experiment were from Jinzhou underground gabbro, based on the sampling core provided by the other party. Choose the core that meets the standard and test design, first cut with a stone saw and then polish the end face with a grinder. Finally, a cylindrical test piece of φ50 mm×100 mm was formed.

(2) Measurement of sample parameters The basic parameters of each test piece are recorded with an accuracy of 0.01 mm vernier caliper, an accuracy of 0.01 g electronic balance, an ultrasonic tester and a digital camera. The length, diameter and weight of the sample were measured and the rock sample density was calculated. Then, the PantitLab ultrasonic detector manufactured by SwissPROCEQ was used to measure the longitudinal wave velocity of the rock, and the average of the multiple measurements was performed. Finally, the data is aggregated to exclude gabbro samples that measure anomalies. The gabbro density is between 3.040 and 3.081 g/cm3, and the average longitudinal wave velocity is 6704 m/s to 6892 m/s.

(3) Experimental procedure The gabbro samples were divided into two groups. The single-axis direct loading was divided into 4 groups for experiments, and the cyclic addition and subtraction experiments were divided into 6 groups. The experimental design has a loading rate of 1000 N/s and an unloading rate of 1000 N/s. First, a single-axis direct loading test was performed, first by stress loading, and then converted to deformation control after reaching 70% rock strength. Until the last damage to the rock breaks, then do as much as possible after the peak remains. The gabbro rock samples were loaded 4 times to determine the uniaxial compressive strength of the gabbro. The strengths of the samples obtained in the 4 experiments were 172 MPa, 177 MPa, 173 MPa and 180 MPa, respectively. Therefore, the uniaxial compressive strength of the gabbro can be determined. The strength is about 175 MPa. According to the uniaxial compressive strength test of the gabbro sample, the strength of the test piece is 175 MPa to design the cyclic addition and unloading of the gabbro. For the cyclic addition and unloading experiments, the design scheme is shown in Figure 1. The sample was first loaded to 60% uniaxial strength. The design load is 210kN and then drops to 10% of the sample strength, which is planned to be 40kN. A 6-component gradient experiment was then performed, stepwise loading with a gradient of 20 kN, and the same protocol was offloaded to the same value of the design each time. As the program gradually increases, the unloading value also increases by 20kN. Test the mechanical properties and other parameters of the test piece, and finally analyze and compare the parameters.

4.2 Comparative Analysis of Results

The effects of different loading conditions on gabbro samples were analyzed and compared with single-axis direct loading. The stress-strain curves of gabbro samples were analyzed in detail through different test results of loading and unloading, and the effects of various loading schemes on the strength of the specimens were analyzed. Combined with uniaxial loading and cyclic addition and unloading of samples, the accuracy of the verification results was analyzed.

Table 1: Uniaxial compression sample parameters

Sample Number	Density/g.cm^{-3}	Wave Speed/m.s^{-1}	Strength/MPa	E/GPa	E_{50}/GPa
DZ-1	3.047	6888.01	172	126.4	124.4
DZ-2	3.060	6877.35	177	125.0	124.6
DZ-3	3.056	6768.83	173	105.0	103.4
DZ-4	3.051	6852.74	180	115.0	113.9
Average Value	3.053	6846.73	175	117.8	116.6

ISSN 2706-655X Vol.3, Issue 9: 56-65, DOI: 10.25236/IJFET.2021.030910

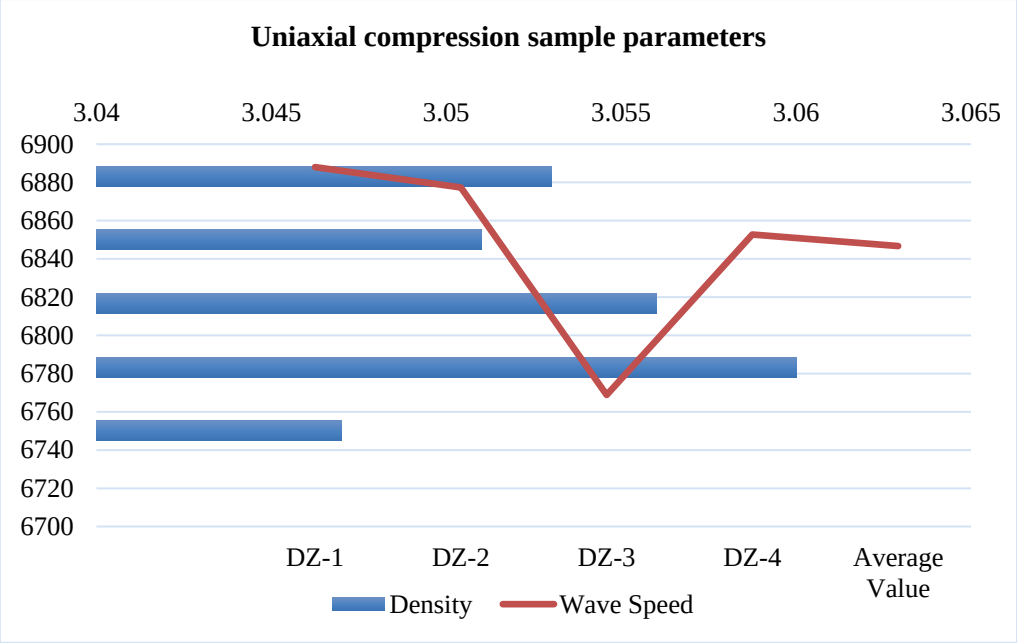

Figure 1: Uniaxial compression sample parameters

(1) Uniaxial direct loading mechanical parameters Figure 1 shows the uniaxial compressive strength stress-strain curves of typical gabbro samples. The stress and axial strain are substantially linear before the peak reaches the peak. When the test piece is damaged by force, the load bearing capacity will be temporarily lost. After compression, the residual strength of the sample will appear after the peak. After the uniaxial direct loading experiment, the average elastic modulus of the gabbro shown in Table 1 (ie, the approximate slope of the straight line on the stress-strain curve), the secant modulus E_{50} (origin and stress-strain curve 50%) were obtained. The slope of the compressive strength point line), the uniaxial compressive strength and the average bearing capacity after the uniaxial peak. It can be seen from the data in Table 1 that the density and wave velocity of the gabbro sample are relatively large, indicating that the rock interior is relatively compact and has a higher compressive strength. After uniaxial direct loading, it can be seen that the elastic modulus of the gabbro sample is relatively large, and the elastic modulus is an important index to measure the degree of deformation of the material. The larger the value of the gabbro sample, the smaller the elastic deformation of the test piece, the higher the stiffness and the stronger the brittleness. This indicates that the previously measured sample data is consistent with the uniaxial loading experiment.

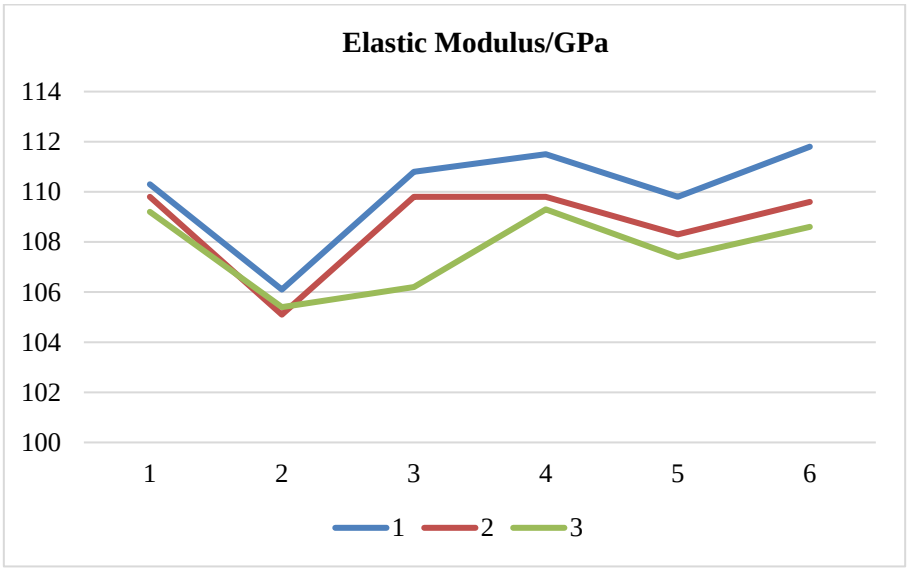

Figure 2: Comparison of elastic modulus

ISSN 2706-655X Vol.3, Issue 9: 56-65, DOI: 10.25236/IJFET.2021.030910

(2) Mechanical properties of cyclic loading and unloading According to the design of six different cyclic loading and unloading schemes, the mechanical parameters of the gabbro samples shown in Table 1 were obtained. It can be seen from Table 1 that the compressive strength of the cyclic loading and unloading test pieces of different schemes does not change regularly, but the average peak intensity of cyclic loading and unloading reaches 192 MPa. The average peak intensity of cyclic loading and unloading increased by 10% compared to the average strength of 175 MPa for single-axis direct loading. In this case, it may be that the internal cracks of the test piece overlap each other, so that the test piece is more encrypted as a whole. It has better load carrying capacity, and cyclic addition and unloading enhances the peak strength of the gabbro. The cyclic loading and unloading experimental scheme designed in this paper first loads the sample to 60% of the strength of the sample, and then performs continuous cyclic loading and unloading in the middle until the last loading causes the sample to be destroyed. The goal is to get the same test. As shown in Table 1, the average modulus of elasticity of the first gabbro sample was E\u003d109.49 GPa, and the average modulus of elasticity of the last loaded sample was 107.7 GPa. The average elastic modulus of the first test piece was reduced by 2%, indicating the addition and unloading of gabbro during the cycle. The influence of the elastic modulus of the test piece still has a certain influence. Under the same force conditions, the axial load of the test piece will be slightly larger than the original first load compared to the first load. The results show that for gabbro samples, cyclic loading and unloading also soften the strain. Figure 2 shows the damage of the sample after the addition and unloading of the gabbro sample. Most specimens are mainly in the form of split failures. During the process of adding and unloading gabbro samples, it is actually a process of repeating work between the rock sample and the press. In addition, the work of adding and unloading is not equal, indicating an energy loss. The rock sample is actually compacted at the beginning of the loading and unloading cycle and will have a crack closed after the internal force of the rock sample. So at the beginning, it took a lot of power. As the applied force continues to increase, the gabbro sample begins to enter the yield phase, and the energy consumption during the yield phase will be large, accompanied by damage to the specimen. When it is destroyed, it produces a huge noise, accompanied by the release of energy.

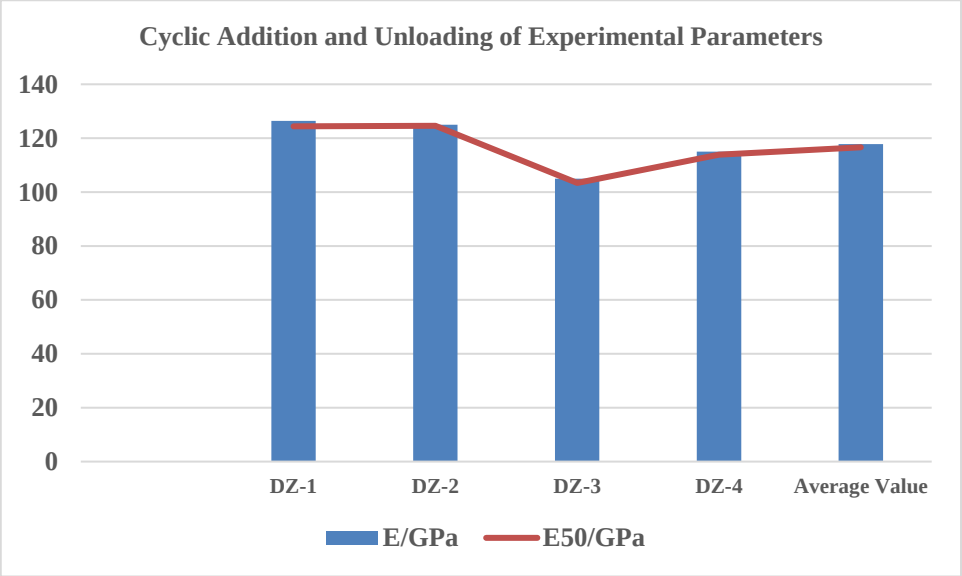

Figure 3: Shows the damage of the sample

After the addition and unloading of the gabbro sample. Most specimens are mainly in the form of split failures. During the process of adding and unloading gabbro samples, it is actually a process of repeating work between the rock sample and the press. In addition, the work of adding and unloading is not equal, indicating an energy loss. The rock sample is actually compacted at the beginning of the cyclic loading and unloading, and the rock sample breaks after being subjected to internal pressure: the gap is closed, so it needs to consume a lot of power at the beginning. As the applied force continues to increase, the gabbro sample begins to enter the yield phase, and the energy consumption during the yield phase will be large, accompanied by damage to the specimen. When it is destroyed, it produces a huge noise, accompanied by the release of energy.As shown in Figure 3.

ISSN 2706-655X Vol.3, Issue 9: 56-65, DOI: 10.25236/IJFET.2021.030910

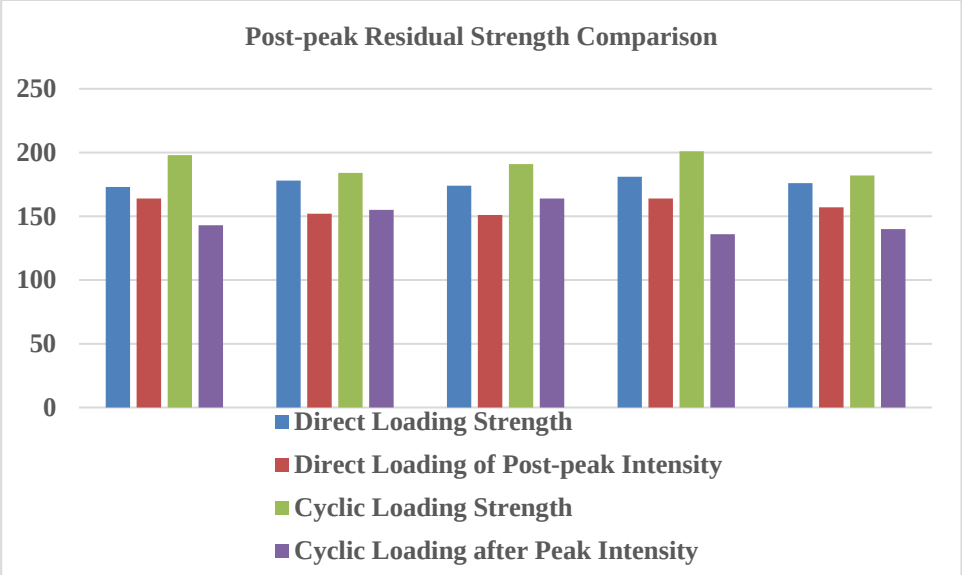

Figure 4: Comparison of residual strength after peak

After uniaxial loading, the residual strength decreased by 11.6% after direct loading, and the uniaxial direct loading strength was 175 MPa compared with gabbro samples. After cyclic addition and unloading of the peaks, the residual strength was reduced by 22.2% compared to the gabbro samples. After cyclic addition and unloading of peaks, the residual strength was reduced by 34%. The cycle addition and unloading were 9.5% lower than the residual strength after uniaxial direct loading. It can be seen from the calculation that although gabbro is cyclically added and unloaded, the effects of cyclic addition and unloading on gabbro samples are still very large. Its strength is improved, but when the sample is broken, its post-peak bearing capacity will be more obvious. If it is associated with engineering practice, the rock mass will reduce the rock carrying capacity after repeated loading and unloading.As shown in Figure 4.

5. Conclusions

(1) The rock slurry increases with the increase of the axial compression load of the next stage. The strength of the rock slurry under loading and unloading is higher than that of the conventional triaxial, mainly due to the fact that the circulation under low stress conditions makes the test piece more dense.

(2) Under cyclic loading and unloading conditions, the fracture strength of rock slurry generally shows an increase in particle size and a decrease in fracture strength. The particle size contact in the coarse-grained rock slurry has more space than the fine-grained rock slurry, and the coupling effect between the particle sizes is not good, and the damage is more likely to occur.

(3) The failure of rock slurry under cyclic loading and unloading conditions is mainly in the form of shear failure. The increase of the particle size of the rock does not change the failure mode of the rock slurry. It is difficult to shear the rock particles of the shear surface in the shear failure of the rock slurry. The rock particles will reverse under the shear stress, thus driving around the shear surface. The destruction forms a shear band. The larger the particle size of the rock particles, the larger the range of shear bands. Based on the research results, in the grouting reinforcement of soft rock, the key techniques to improve the prestress of the anchor and increase the grouting effect are proposed.

Acknowledgements

This work was supported by The National Natural Science Foundation of China (41602154) and Projects of Talents Recruitment of GDUPT (2018rc01)

References

[1] Wang, X. X., Ma, W. J., Huang, J. W., & Liao, Z. Y. (2014) "Mechanical Properties of Sandstone

ISSN 2706-655X Vol.3, Issue 9: 56-65, DOI: 10.25236/IJFET.2021.030910

under Loading and Unloading Conditions", Advanced Materials Research, 852(1), pp. 441-446.
[2] Imole, O. I., Wojtkowski, M., Magnanimo, V., & Luding, S. (2014) "Micro-macro Correlations and Anisotropy in Granular Assemblies under Uniaxial Loading and Unloading", Physical Review E Statistical Nonlinear & Soft Matter Physics, 89(4), pp.042210.
[3] Koniorczyk, M., Gawin, D., & Schrefler, B. A. (2015) "Modeling Evolution of Frost Damage in Fully Saturated Porous Materials Exposed to Variable Hygro-thermal Conditions", Computer Methods in Applied Mechanics & Engineering, 297(3), pp. 38-61.
[4] Zeng, Z., & Tan, J. C. (2017) "Afm Nanoindentation to Quantify the Mechanical Properties of Nano- and Micron-sized Crystals of A Metal-organic Framework Material", Acs Appl Mater Interfaces, 9(45), pp.39839-39854.
[5] Bi, L., & Pan, G. (2014) "Facile and Green Fabrication of Multiple Magnetite Nano-cores@void@porous Shell Microspheres for Delivery Vehicles", Journal of Materials Chemistry A, 2(11), pp.3715-3718.
[6] Liu, X. R., Liu, J., Dong-Liang, L. I., Chun-Mei, H. E., Wang, Z. J., & Xie, Y. K. (2017) "Experimental Research on the Effect of Different Initial Unloading Levels on Mechanical Properties of Deep-buried Sandstone", Rock & Soil Mechanics, 38(11), pp. 3081-3088.
[7] Mehdizadeh, S. (2014) "Profiles and Projections of Ohio's 60 Population: County-By-County", Journal of Materials Science, 49(1), pp. 163-179.
[8] Liang, Y., Li, Q. , Gu, Y. , & Zou, Q. . (2017) "Mechanical and Acoustic Emission Characteristics of Rock: Effect of Loading and Unloading Confining Pressure at the Postpeak Stage", Journal of Natural Gas Science and Engineering, 44(3), pp. 54-64.
[9] Dong, X., Tian-Hong, Y. , Pei-Tao, W. , Peng-Hai, Z. , & Yong-Chuan, Z. . (2014) "Experimental Study of Acoustic Emission Characteristics of Dry and Saturated Rocks during Cyclic Loading and Unloading Process", Journal of China Coal Society, 39(7), pp.1243-1247.
[10] Therefore. (2018) "Mechanical Behavior of Shale Rock under Uniaxial Cyclic Loading and Unloading Condition", Advances in Civil Engineering, 2018(3), pp.1-8.
[11] Huo, L., Zhou, Y., Yang, C. H., Mao, H. J., Liu, J. X., & Chen, X. L. (2017) "Experimental Study of Unloading Mechanical Behaviour of Mudstone in Different Geological Era", Rock & Soil Mechanics, 38(3), pp. 714-722.